Colloid Polym Sci 275:234–243 (1997)

ORIGINAL CONTRIBUTION

C. Baehr
B. Glüsen
J.H. Wendorff
E.G.J. Staring

Pockels-effect relaxation in poled side chain polymers: Decoupling of chromophor reorientation from α-relaxation

Received: 1 August 1996
Accepted: 22 November 1996

Dr. C. Baehr (✉) · B. Glüsen
J.H. Wendorff
Fachbereich Physikalische Chemie
Wissenschaftliches Zentrum
für Materialwissenschaften
Philipps-Universität Marburg
35032 Marburg, Germany

E.G.J. Staring
Philips Research
5600 JA Eindhoven, The Netherlands

Abstract The relaxation of the polar order of poled side chain polymers carrying NLO-active chromophores was monitored by Pockels-effect relaxation studies. Dielectric relaxation investigations were performed in order to analyze the coupling or decoupling of the chromophore reorientation to the relaxation modes of the side chain polymers. It was found that the chromophores perform their own reorientation relaxation mode both in the molten and the glassy state, which is not coupled to backbone relaxations. The chromophore reorientation process is characterized by a narrow distribution of the relaxation times and high activation energies. Studies on physical aging reveal that the chromophore reorientation is controlled by the free volume. The chromophore reorientation process can be influenced by the chemical linkage of the chromophore to the polymer backbone and by the nature of the backbone.

Key words NLO materials – Pockels-effect – dielectric relaxation spectroscopy – physical aging – amorphous side chain polymers

Introduction

Polymers containing side groups characterized by a large hyperpolarizability ß have recently met with considerable interest regarding their application in the area of frequency doubling (SHG) and electro-optical (Pockels-effect) modulations [1–5]. A basic requirement for such application is the absence of an inversion symmetry not only for the chromophores (i.e. on a molecular level) [6] but also on the macroscopic scale [7].

The introduction of a non-centrosymmetric order is achieved, for instance, by applying an electric field to the amorphous side chain polymers in their viscous state and by subsequently freezing-in the polar order by cooling down to the glassy state. The polar order thus introduced is not stable even at temperatures well below the glass transition temperature but relaxes within time scales which vary between minutes and years. The relaxation is fast when close to the glass transition temperature and slows down with decreasing temperature.

Experiments, which are sensible to $\chi^{(2)}$, are appropriate tools to observe the polar order [8]. Investigations have shown that both the introduction of cross-links [9] or the polymerization after poling [10] and the use of selected polymer backbone structures [11–13] can lead to high glass transition temperatures which in turn reduce the tendency towards the decay of orientation of the chromophore and thus the decrease of the NLO-activity.

Several studies were concerned in the past with the characterization of the molecular origin of this relaxation [14–29]. Kuzyk et al. [14] introduced the picture that the chromophore reorientation is restricted to the voids formed by excess free volume of the polymer matrix. Besides that, the chromophores have only weak interactions with the cage around them. This picture was refined [18, 27, 28] and formulated in a more quantitative way by interpreting the reorientation as rotational Brownian motion of the

chromophores [24]. Consequently, the order parameter and the reorientation dynamic of the chromophores were used to describe the elastic response on a microscopic scale [14, 18, 27] and the free volume [24] respective the activation volume [28]. Wang et al. [26] proposed that this mechanism characterizes the short-time regime of the chromophore reorientation whereas cooperative motions of the matrix change position and orientation of the confining voids and thus characterize the long-time regime. A different picture involves large-scale cooperative motions of the matrix polymer only [15–17, 20–22, 29].

An important question is the coupling of the mobility of the chromophore to the modes of matrix mobility. Does it couple to secondary relaxations taking place in the glassy state, for example, the γ-relaxation as proposed by Qui et al. [23] based on the examination of photoisomerization in a PMMA matrix? Or does it couple to the glass relaxation (α-process), which involves cooperative large-scale motions? This interpretation was given by Dhinojwala et al. [21, 22] based on the comparison of SHG and dielectric relaxation experiment data and was also proposed by other groups qualitatively [15–17, 29]. Or do the chromophores perform a motion independent from the relaxations mentioned above?

This contribution deals with the evaluation of the molecular motions which cause the relaxation of the NLO-activity in selected amorphous side chain polymers. The aim is to describe in detail the molecular motions involved, their dependence on free volume as well as on the chemical structure of the polymer backbone and the chemical linkage of the chromophores to the backbone. We applied a combination of different techniques: For the observation of chromophore reorientations, the Pockels-effect relaxation is a suitable tool especially at lower temperatures respective longer relaxation times. Dielectric relaxation studies are used to study relaxation modes of both, the polymer matrix and the chromophore at higher temperatures respective shorter relaxation times. The analysis of aging effects gives evidence to the role of free volume.

Experimental section

Materials

The experiments were performed on different types of polymers carrying NLO-active side groups. Scheme 1 represents their chemical structures, the synthesis has been described elsewhere [30, 31]. The polymers differ with respect to the nature of the backbone (polyurethane, polymethylmethacrylate), the coupling of the side groups to the backbone (with and without a spacer) as well as with respect to the position of the SO_2-dipole displaying a large component parallel to the long axis of the chromophore.

All polymers are amorphous, the glass transition temperatures were measured in a Perkin-Elmer DSC-7 using a 20 K/min heating rate. The glass temperatures were taken as the mid-point of the heat capacity step. The refractive indices at 632.8 nm and room temperature were obtained from a HeNe-laser equipped Metricon 2000 prism coupler. The effective chromophore content, the thermodynamic data and the refractive indices are listed in Table 1.

Scheme 1 Chemical structure of compounds

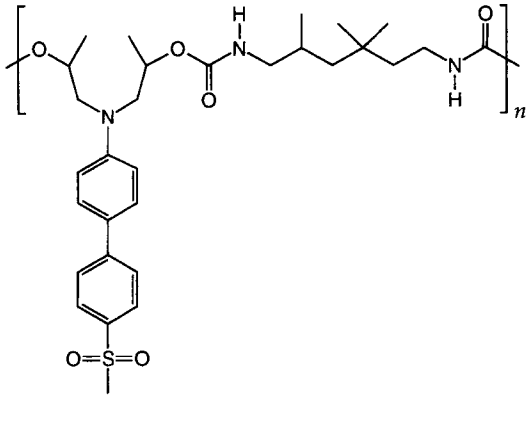

A

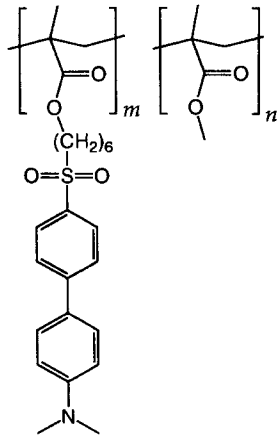

B: m/n = 38/62
C: m/n = 17/83

Colloid & Polymer Science, Vol. 275, No. 3 (1997)

Table 1 Effective chromophore amount, calorimetric data and refractive indices

Compound	x^* [wt%]	T_g [°C] (DSC 20 K/min)	Δc_p [J/mol K] (DSC 20 K/min)	n (at 632.8 nm)
PMMA	0	88	0.33	1.4855
A	47	101	0.37	1.5831
B	46	81	0.34	1.5835
C	30	97	0.36	1.5504

Sample preparation

For Pockels-effect relaxation studies, the samples were moulded between two glass supports coated with transparent ITO-electrodes (Baltracon Z20). The sample thickness was adjusted by using 25 μm-spacers of polyimide (Kapton). The samples for the dielectric measurements were prepared either by moulding or by spincoating. In both cases polished and gilded electrodes from stainless steel were used. When moulded, a sample thickness of 50 μm was maintained by glass fibers (Schott & Söhne). For spincoating about 10 wt% polymer were dissolved in spectroscopic-grade chlorobenzene and spincoated on a 25 mm diameter electrode. After drying on a hot plate for a couple of minutes first and for 24 h at 150 °C *in vacuo* later, the samples were sputtered with a 700 nm Au-layer of 5, 10 or 20 mm diameter depending on the sample thickness.

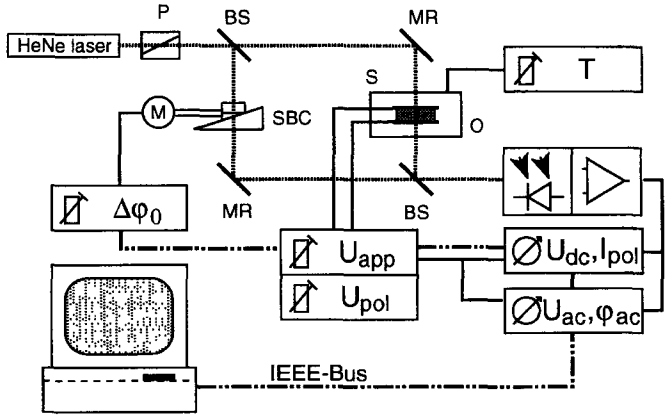

Fig. 1 Pockels setup. SBC: Soleil Babinet compensator, M: step motor, P: polarizer, BS: beam splitter, MR: mirror, S: sample, O: oven, $\Delta\phi_0$: constant phase difference (working point), U_{app}: applied modulation voltage, U_{pol}: poling voltage, T: temperature, U_{ac}: ac part of output voltage, U_{dc}: dc part of output voltage, I_{pol}: poling current, ϕ_{ac}: phase difference between modulation voltage and ac part of output voltage

Pockels measurements

The Pockels-effect was measured with the experimental setup shown in Fig. 1. The principal part is a Mach Zehnder interferometer with the sample in one of its two branches. The periodically modulated electric field applied to the sample induces a phase shift along one path of the interferometer and thus a modulation of the output intensity. The AC output voltage of the detector preamplifier is monitored by a Lock-in amplifier. Its amplitude is a measure of the phase shift and thus of the Pockels coefficient. In addition, the DC output voltage was monitored to detect any working point drift during an experiment which could take days. By using the Soleil Babinet compensator a constant phase shift of $\pi/2$ was maintained. We analyzed the Pockels coefficient r_{13}.

After being kept at 30 K above their glass temperature for 1 h to erase the thermal history the samples were poled in a field of 10 V/μm at 15 K above their glass temperature for 30 min. The field strength is low as opposed to what is used for efficient poling to ensure comparability of the Pockels and dielectric measurement results. After cooling down rapidly and stabilizing at the desired temperature, which took altogether less than 5 min, the poling field was removed and the relaxation of polar order at constant temperature was determined. The electrodes were effectively short-circuited due to the low internal resistance of the AC modulating voltage source. For studies on aging the samples were kept at the selected aging temperature for the selected aging time before removing the poling field and measuring the decay of polar order as described above.

Dielectric measurements

An automatic bridge (Hewlett-Packard 4284A) was used to analyze the dielectric behavior. The temperature range amounted to −170 °C and 200 °C and the frequency range from 20 Hz to 1 Mhz. Some measurements at very low frequencies down to 10^{-2} Hz were made at the Max-Planck-Institute for Polymer Research Mainz using a frequency response analyzer (Schlumberger Solartron 1254) equipped with a high-impedance buffer amplifier. The detailed measurement setups have been described elsewhere [32].

Results and discussion

Relaxation of the magnitude of the Pockels coefficient

The Pockels coefficient r_{13} was measured at constant reference temperature as a function of the time since switching off the poling field. Figure 2 displays characteristic decay curves as obtained for the polymer B for various temperatures. The coefficient decreases for shorter times and approaches almost zero for sufficiently long times, the residual nonlinear optical effect was less than 2% of the initial value. It is also evident that the relaxation is not characterized by a single relaxation time but rather by a relaxation time distribution. Polymer A shows a similar behavior.

The evaluation of the relaxation time distributions meets with problems. A biexponential function as proposed by Hampsch et al. [16] and Wang et al. [25] for guest–host systems could definitely not be fitted to our experimental data. We fitted both, Kohlrausch–William–Watt (KWW) functions [33–35] and decay functions, which results from a logarithmic normal distribution of relaxation times:

$$\tau g(\ln \tau) = \exp\{-[\ln(\tau/\tau_g)]^2/\sigma^2\}/\sqrt{2\pi\sigma^2}\,. \quad (1)$$

KWW functions have been used in the past for guest–host systems [20–22, 28, 29] for main-chain polymers [25] and for side-chain polymers [20–22, 25, 26, 28, 29]. They can be interpreted as the result of a relaxation time distribution [36] as well as hierarchical or constraint processes [37, 38]. A logarithmic normal distribution of relaxation times was proposed by Schüssler et al. [39] and their interpretation is straightforward: The logarithmic normal relaxation time distribution originates from a Gaussian distribution of energy barriers of activated processes [40, 41]. A maximum data rate of one measurement per 15 s restricted the accuracy of the fitting in the regime of very short times where the main differences between the two decay functions occur. However, decay functions of logarithmic normal relaxation time distributions fitted the data better. In addition, there was no need to express very long relaxation modes by a constant as proposed by Wang et al. [26]. In the following, we will discuss both the effect of temperature variations on the mean relaxation time as well as on the relaxation time distribution.

Figure 3 displays the influence of a temperature increase on the mean relaxation time for the different polymers studied: the relaxation rate increases strongly with increasing temperature. This analysis reveals that the relaxation process is thermally activated, which confirms the findings of Dhinojwala et al. [20–22] and Hooker et al. [29]. Yet the activation energy of the Pockels-effect relaxation is unusually large. It amounts to 257 ± 12 kJ/mol for polymer A and to 331 ± 25 kJ/mol for polymer B compared to values around 50 kJ/mol reported by them. Secondary relaxations occurring in the glass state – such as, for example, side group rotation of polyacrylates or polymethacrylates – are also known to follow an Arrhenius behavior [42–44] but they have activation energies between 50 and 70 kJ/mol and mean relaxation times roughly six decades shorter than the ones of the Pockels-effect relaxation.

A second characteristic feature of this relaxation is that the width of the relaxation time distribution decreases

Fig. 2 Decay of nonlinear optical activity of B, not aged, normalized to the extrapolated at $t = 0$ s and $t = \infty$: (——) 87 °C, (– – –) 82 °C, (· · · · · ·) 77 °C, (— — —) 72 °C, (– · · –) 67 °C

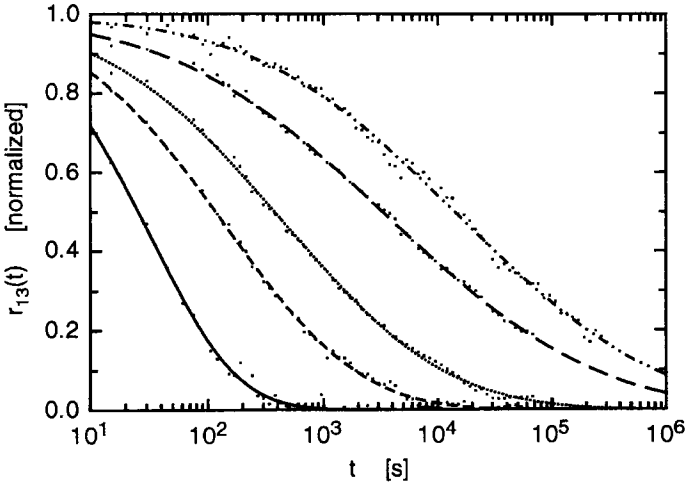

Fig. 3 Arrhenius diagram of mean relaxation times: (▲) A, (▼) B, (△ and ▽) calorimetric glass temperatures

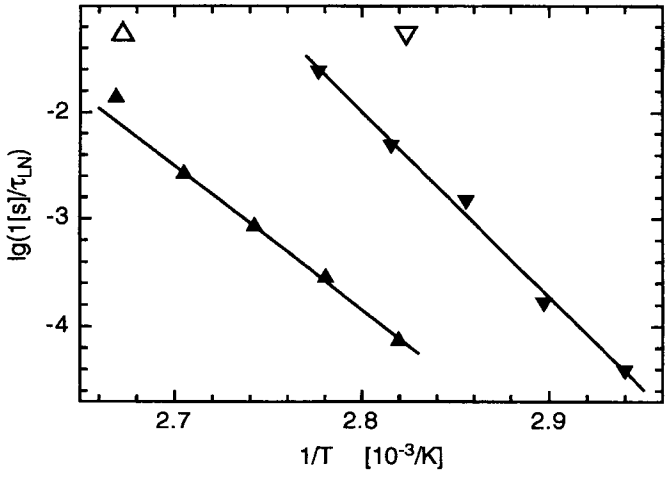

strongly with increasing temperature and seems to approach almost the case of a single relaxation time at a temperature slightly above the glass transition. Figure 4 gives an example for the change in distribution with increasing temperature for the polymer B. Similar results were obtained for the other polymers studied. Again these features differ from the known behavior of secondary relaxations in glassy polymers. Our conclusion is that the chromophore relaxation apparently does not couple to secondary motions.

The mean relaxation times obtained at temperatures around the calorimetric glass transition temperature are about one decade longer than the ones expected for the α-relaxation based on WLF-calculations as shown in Fig. 3. This fact together with the narrow relaxation time distribution around glass temperature indicates that there is no genuine coupling of the chromophore relaxation to glass relaxation.

Aging effects

Physical aging is known to originate from the relaxation of the nonequilibrium glassy state at a given aging temperature towards the corresponding equilibrium state determined by extrapolating the molten state to this aging temperature. Aging is connected with the relaxation of enthalpy, volume and also of free volume [45–48]. It can thus be monitored directly, for instance, by following volume changes in dilatometry or enthalpy changes in calorimetry. The relaxation of the free volume strongly effects all relaxations depending on it. Analyzing physical aging in such NLO side-chain polymers is one possible method to find out whether the Pockels-effect relaxation is controlled by free-volume effects.

The first step of the evaluation of physical aging consisted in the calorimetric evaluation of the enthalpy relaxation: The purpose was to find out if physical aging in polymers with high concentration of bulky and dipole carrying groups occurs along similar lines as in polymers such as polyacrylates or polymethyl-methacrylates with smaller side groups. The DSC-curves on unaged and aged samples show beyond any doubt that all side chain polymers discussed here are able to age. The different polymers display different aging rates, yet the calorimetrically observed aging rates are within the range found for amorphous polymers in general.

Figure 5 shows the effect of annealing polymer A at a given aging temperature in the presence of the poling field on the relaxation of the Pockels-effect. It is apparent that the relaxation is strongly slowed down with increasing aging time. The logarithmic shifts of the mean relaxation times is plotted versus the aging time in Fig. 6. This continuous shift of the relaxation time with increasing aging time is characteristic for physical aging. Thus, the Pockels-effect relaxation is controlled by free volume. The aging rates are in the same range as the ones reported by Dhinojwala et al. [21, 22] but for lower aging temperatures.

The analysis of the relaxation time distribution reveals that the width of the distribution remains constant. Such behavior has been named "rheologically simple". Each individual relaxation within the relaxation time distribution is shifted along the time scale with the same factor. Similar results were obtained for all polymers studied and confirm the findings of Dhinojwala et al. [22]. There is

Fig. 4 Relaxation time distribution of chromophor reorientation of B, not aged: (——) 87 °C, (– – –) 82 °C, (· · · · · ·) 77 °C, (— — —) 72 °C, (— · —) 67 °C

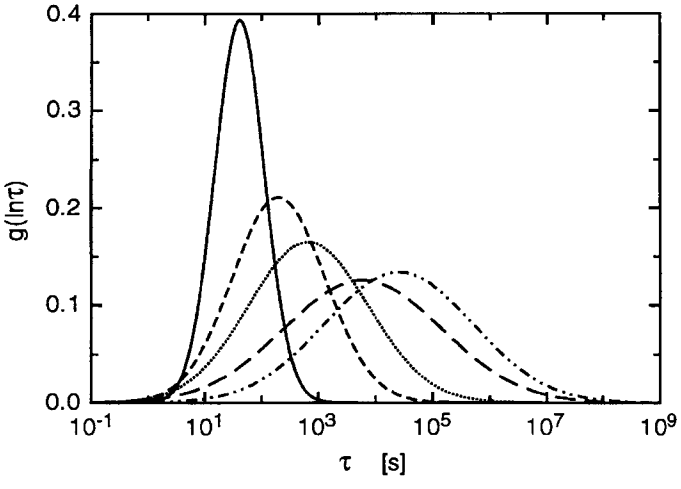

Fig. 5 Decay of nonlinear optical activity of A aged at 91.5 °C, normalized to the extrapolated at $t = 0$ s: (——) 0 min, (– – –) 60 min, (· · · · · ·) 120 min, (— — —) 300 min, (— · —) 810 min

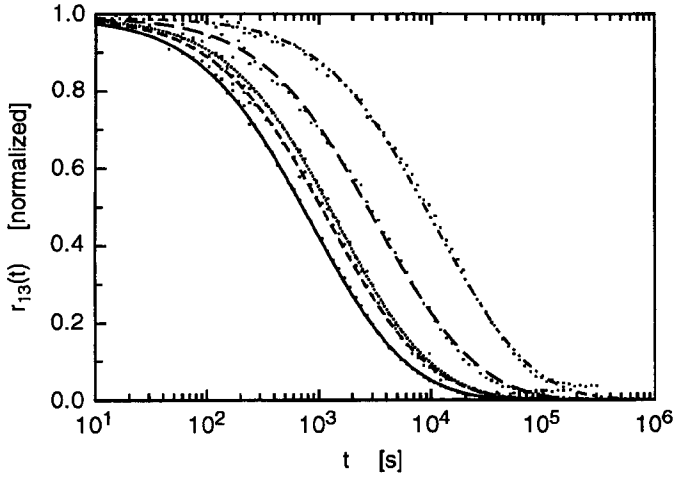

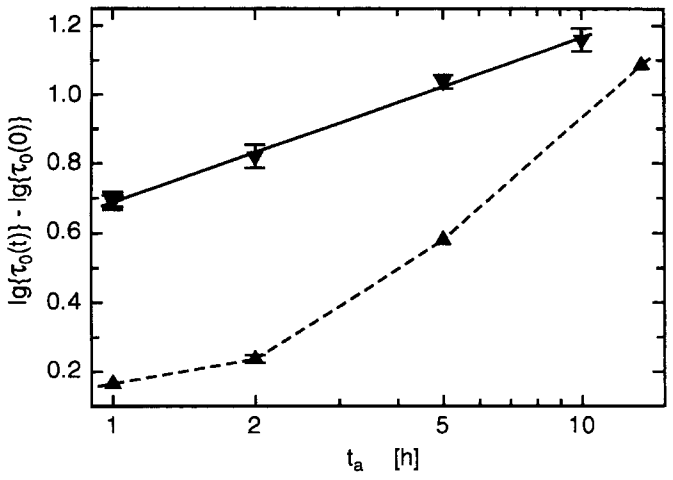

Fig. 6 Aging rates of Pockels aging experiments on (▲) A and (▼) B

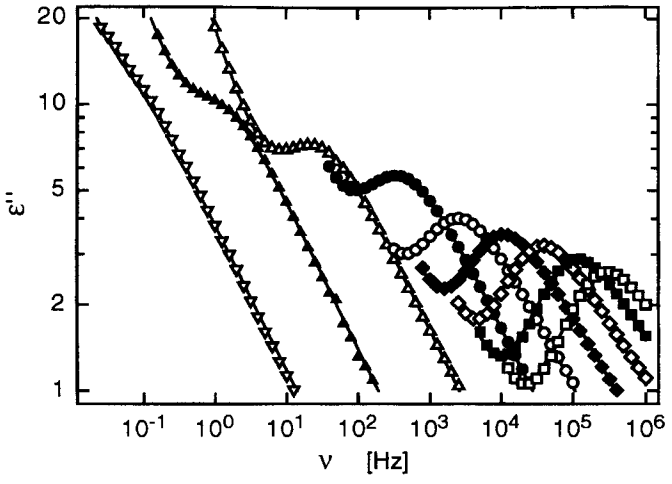

Fig. 7 Imaginary part of dielectric function of A: (□) 190 °C, (■) 180 °C, (◇) 170 °C, (◆) 160 °C, (○) 150 °C, (●) 140 °C, (△) 130 °C, (▲) 120 °C, (▽) 111 °C

a sharp contrast to the increase of KWW-parameter β with pressure reported by Brower et al. [28] although pressure-dependent measurement should lead to the same results. This difference may come from the limited time scale of their decay experiments as well as from the fact, that they did the experiment above T_g.

Results of dielectric relaxation investigations

The homopolymer PMMA displays a secondary relaxation characterized by a constant activation energy of 65 kJ/mol which is in good accordance with literature [42–44]. It has been attributed predominantly to side group motions which couple to a certain extent to main chain torsional motions [49]. The low-frequency relaxation corresponds to the glass relaxation. It follows a WLF-behavior [50] and the extrapolation of the WLF curve to low frequencies (0.01 Hz) yields a glass transition temperature which agrees with the one observed by calorimetry.

The NLO-polymers considered here are also characterized by the occurrence of secondary relaxations at high frequencies and with constant activation energies between 30 and 100 kJ/mol. An important result is that the relaxation strengths of the secondary relaxations are very weak, which excludes high-frequency motions of the side group chromophore carrying the strong SO_2-dipole.

At lower frequencies the NLO-active polymers display a process (Fig. 7) carrying most of the relaxation strength which is of the order of 5–10. Clearly, this relaxation process is connected to large-scale chromophore motions which is substantiated by theoretical calculations [51].

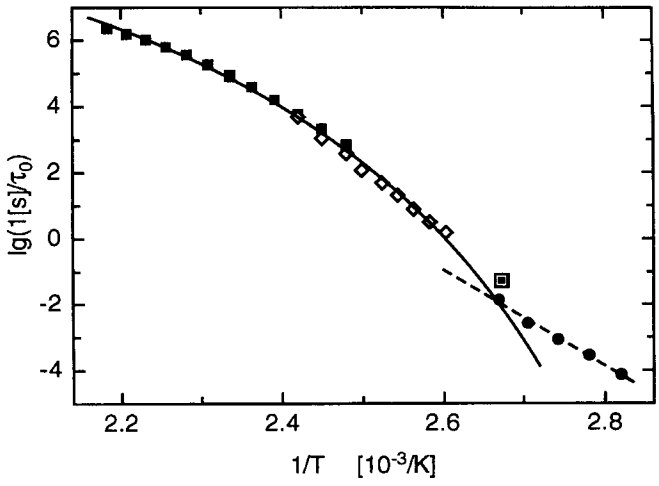

Fig. 8 Arrhenius diagram of dielectric relaxation and NLO decay of A Chromophor relaxation: (■) τ_0 from HN-fit, (◇) low-frequency experiment, (——) WLF fit. NLO decay: (●) mean relaxation times, (– – –) Arrhenius fit. (■) calorimetric glass transition

This relaxation process has some peculiar features. First of all it displays a WLF-type frequency-temperature superposition shown for the polymers A and B in Figs. 8 and 9. Yet, the extrapolation of this activation curve to lower frequencies does not yield the calorimetrically determined glass transition temperature. The extrapolated temperature may be either far from the quasi-static location of the glass transition (Fig. 9) or closer to it (Fig. 8). A second interesting feature is the narrow width of the relaxation time distribution, as obtained on the basis of a Havriliak Negami analysis [52]. This is obvious from the comparison of distributions displayed in Fig. 10. The dielectric

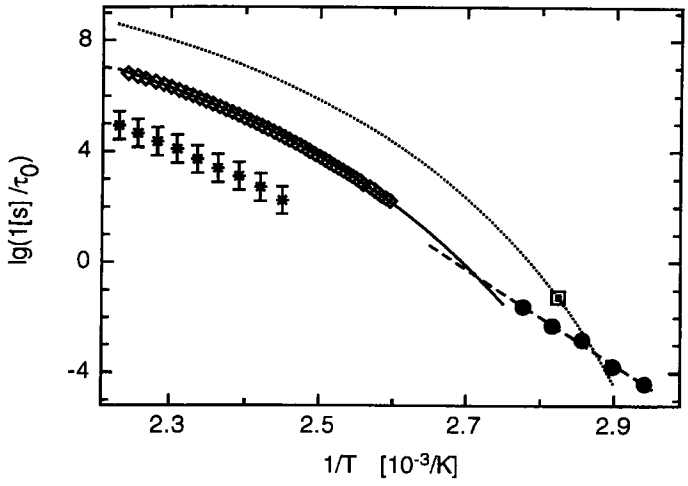

Fig. 9 Arrhenius diagram of dielectric relaxations and NLO decay of B Chromophor relaxation: (◇) ν_{max} from tan(δ) , (——) WLF fit. α-relaxation: (·····) WLF curve with theoretical parameters [50], unknown relaxation: * estimated from distance to δ-relaxation NLO decay: (●) mean relaxation times, (– – –) Arrhenius fit. (■) calorimetric glass transition

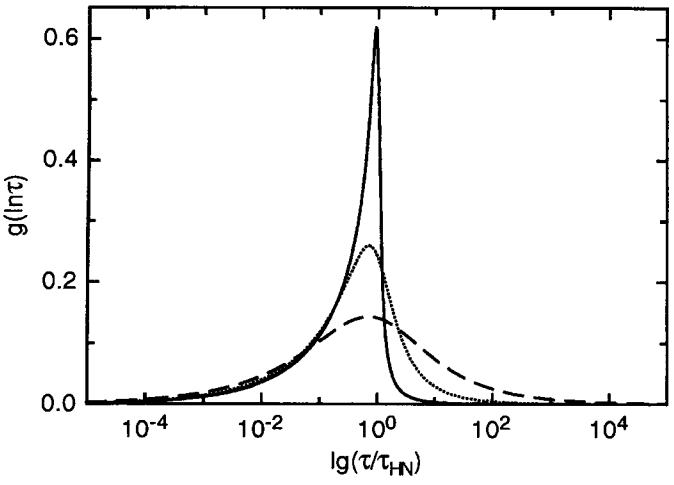

Fig. 10 Relaxation time distributions of dielectric α- and Chromophor relaxation (average distribution parameters from HN-fits of measurements at temperatures between 30 and 50 K above the respective calorimetric glass transition temperature) (——) A, (·····) B, (– – –) PMMA

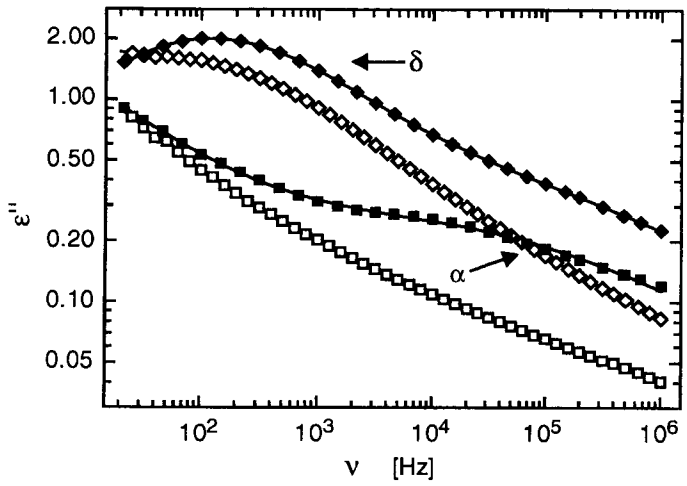

Fig. 11 Imaginary part of dielectric function of B and C B: (□) 95 °C, (◇) 120 °C, C: (■) 110 °C, (◆) 130 °C, (——) HN fits

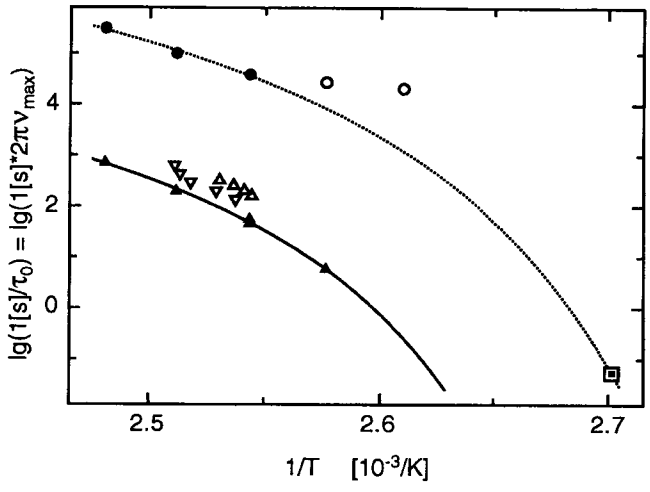

Fig. 12 Arrhenius diagram of dielectric relaxations of C Chromophor relaxation: (▲) τ_0 from HN fit, (▽) and (△) ν_{max} from tan(δ), different preparation, (——) WLF fit α-relaxation: (●) , (○) τ_0 from HN fit, (– – –) WLF fit (based on (●) and (■)). (■) calorimetric glass transition

relaxation behavior described above is not unique, we have observed qualitatively similar results for all other systems studied as described previously [51]. All polymers show a slow relaxation which is not connected to the glass relaxation and which carries a large relaxation strength, all possess narrow relaxation time distributions and all show a WLF-behavior.

The slow relaxation process described above for the NLO-active side group polymers is obviously not identical to the glass relaxation despite the WLF-behavior. The extrapolation to low frequencies is at variance with this. The relaxation strength of the glass relaxation itself seems to be so small that it is masked by the chromophor relaxation in case of polymer B. The α-relaxation can, however, be detected as well as the chromophor relaxation for the side group polymer C, which has a low concentration of the NLO-active side groups. This is apparent from the comparison of the imaginary part of the dielectric functions shown in Fig. 11. Figure 12 displays the activation diagram of the polymer C.

This differs from the experimental data obtained by Dhinojwala et al. [20–22] and their interpretation. One reason could be the fact, that they examined guest–host systems and a side-group polymer, in which the chromophore is attached to the main chain by a very short spacer. The coupling of the chromophore to the chain backbone influences the coupling of the chromophore relaxation to that of the chain backbone i.e. the glass relaxation as evident from the results obtained for the polyurethan: A strong chromophore coupling narrows the frequency gap between the α- and the chromophore relaxation.

The polymer B displays, in addition a second low-frequency relaxation as apparent from Fig. 13. It is characterized by a relatively strong relaxation strength so that it has to be connected with motions of the chromophore. Its location in the activation diagram is shown in Fig. 9. The interpretation of the details of the motions involved is still an unsolved problem.

The low-frequency relaxation process described above has many features in common with the so-called δ-process observed in low molar mass and polymer liquid crystals [53, 54]. The δ-relaxation has been attributed to reorientational motions of the stiff rod-like groups about their small axes; this type of motion involves large-scale reorientational motions in one step up to 180°. The δ-process does not couple to the α-relaxation, the relaxation strength is large ($\Delta\varepsilon = 5$–15 for similar dipole moments), the relaxation time distribution is very narrow approaching the case of a single relaxation time and the activation energy is unusually large in the range of 150 –200kJ/mol. We thus conclude that the chromophore performs similar motions. The only difference is that the relaxation time temperature

Fig. 13 Real part of dielectric function of B (□) 160 °C, (■) 155 °C, (◇)150 °C, (◆) 145 °C, (○) 140 °C, (●) 135 °C, (△) 130 °C, (▲) 125 °C, (▽) 120 °C, (▼) 115 °C

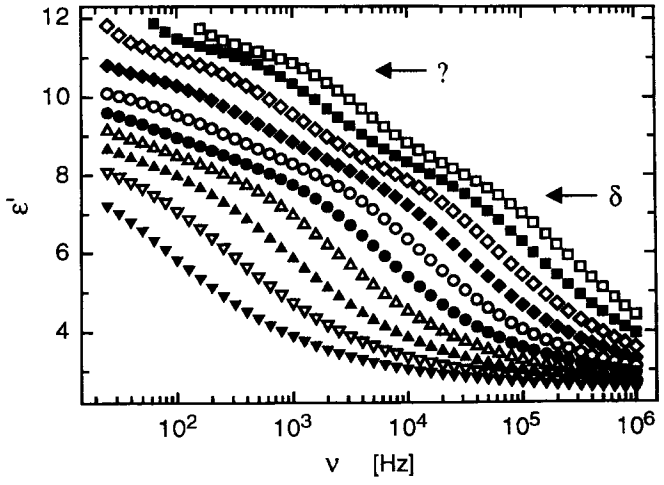

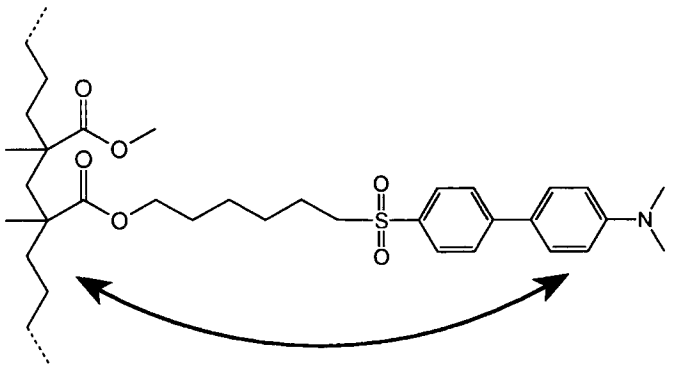

Fig. 14 Schematic mechanism of chromophor relaxation

superposition follows a WLF-behavior for the chromophores and an Arrhenius behavior for the δ-process in liquid crystals. Yet we believe that this difference is not a genuine one since the temperature range in which the liquid crystalline phases exist is too far from the glass transition temperature of low molar mass liquid crystals: The WLF curvature can only be detected beyond any doubt in a temperature range close to the static glass transition [50].

The conclusions which we draw from the dielectric relaxation investigations are as follows: The chromophores do not couple to secondary high-frequency motions taking place in the glassy and molten state nor do they couple directly to the glass relaxation. They perform their own individual relaxation process on a frequency scale up to one order of magnitude smaller than that of the glass relaxation. The process depends on free volume (aging behavior). Its very narrow distribution of relaxation times is apparently caused by a motional averaging process: the fluctuations of the surroundings of the chromophores happen at a time scale which is shorter than the one of the chromophore motion, so the chromophores see an averaged environment. Based on the close correspondence to the δ-process in liquid crystals the chromophore motion is attributed to a large-scale rotational motion approaching at the maximum 180° rotations (Fig. 14).

Conclusions

The chromophore reorientation process of side-chain polymers was studied by monitoring the decay of nonlinear optical activity in a Pockels experiment and by dielectric relaxation measurements to shed some light on the actual type of motion involved. In addition, aging studies were done to explore the dependence of the chromophore reorientation on free volume.

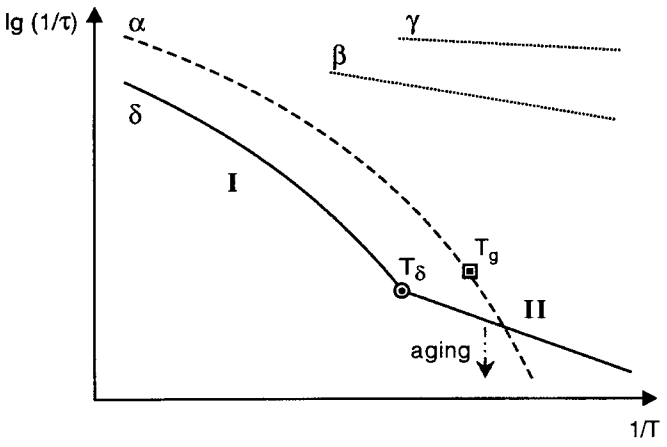

Fig. 15 Schematic relaxation processes of NLO polymers

A main result is that the chromophore side chains of the amorphous polymers studied here perform their own individual mode of motion which is decoupled both from secondary relaxations and from the glass relaxation (Fig. 15). The chromophore motion giving rise to a decay of the NLO-activity takes place both in the molten state and in the glassy state. Its mean relaxation time as well as its relaxation time distribution represented by the width of relaxation time distribution show a continuous transition from high-temperature behavior to low-temperature behavior even in the crossover regime from the fluid to the solid glassy state. The temperature dependence of the mean relaxation time can be described by a Williams–Landel–Ferry behavior above and by an Arrhenius behavior with exceptional large activation energies below a certain transition temperature. Physical aging leads to a retardation of the chromophore reorientation. The chromophore relaxation in the amorphous polymers has many features in common with the δ-relaxation, which is characteristic of rod-like low molar mass and polymer liquid crystals.

The reorientation and the dielectric relaxation of the chromophores are the same process, which involves large-scale rotational motions of the chromophore in one step up to 180°. Above a certain amount of free volume, the reorientation of the chromophores is made possible by cooperative motions of the polymer matrix. At lower-temperatures relaxation modes of the matrix are too slow. The matrix acts like a cage for the chromophore. Overcoming the constraints efforts large activation energies.

The results given above show that aging has a strong effect on the stability of the polar order. The average relaxation time may be increased by several orders of magnitude by aging. A second important parameter which can be used to increase the stability is the location of the glass transition temperature as apparent from the activation diagram shown in Fig. 3. The absolute location of the glass transition temperature controls the location of the activation lines relative to room temperature and thus the relaxation time at room temperature for instance. The expectation based on the activation energies is that an increase of the glass transition temperature by 10 K leads to an increase of the average relaxation time by a factor of about 20.

References

1. Byer RL (1974) Ann Rev Mat Sci 4:147
2. Chen CT, Liu GZ (1986) Ann Rev Mat Sci 16:203
3. Boyd GT (1989) J Opt Soc Am B 6:685
4. Staring EGJ (1991) Recl Trav Chim Pays-Bas 110:492
5. Dalton LR, Harper AW, Wu B, Ghosn R, Laquindanum J, Liang Z, Hubbel A, Xu C (1995) Adv Mater 7:519
6. Lalama SJ, Garito AF (1979) Phys Rev A 20:1179
7. Prasad PN, Williams DJ (1991) Introduction to Nonlinear Optical Effects in Molecules & Polymer. Wiley, Chichester
8. Yariv A (1991) Optical Electronics, 4th ed. Saunders College Publishing, Fort Worth
9. Wright ME, McFarland IE, Hayden LM, Brower SC (1995) Macromolecules 28:8129
10. Zentel R, Baumann H, Scharf D, Eich M, Schönfeld A, Kremer F (1993) Makromol Chem Rapid Com 14:121
11. Kang CS, Heldmann C, Winkelhahn HJ, Schulze M, Neher D, Wegner G, Wortmann R, Glania C, Krämer P (1994) Macromolecules 27:6156
12. Eich M, Beisinghoff H, Knödler B, Ohl M, Sprave M, Vydra J, Eckl M, Strohriegel P, Dörr M, Zentel R, Ahlheim M, Stähelin M, Zysset B, Liang J, Levenson R, Zyss J (1994) Proc SPIE Conf 2285: 104
13. Miller RD, Burland DM, Jurich M, Lee VY, Moylan CR, Thackara JL, Twieg RJ, Verbiest T, Volksen W (1995) Macromolecules 28:4970
14. Kuzyk MG, Moore RC, King LA (1990) J Opt Soc Am B 7:64
15. Hampsch HL, Yang J, Wong GK, Torkelson JM (1990) Macromolecules 23: 3648
16. Hampsch HL, Yang J, Wong GK, Torkelson JM (1990) Macromolecules 23: 3640
17. Köhler W, Robello DR, Dao PT, Willand CS, Williams DJ (1990) J Chem Phys 93:9157
18. Boyd GT, Francis CV, Trend JE, Ender DA (1991) J Opt Soc Am B 8:887
19. Man HT, Yoon HN (1992) Adv Mater 4:159
20. Dhinojwala A, Wong GK, Torkelson JM (1993) Macromolecules 26:5943
21. Dhinojwala A, Wong GK, Torkelson JM (1994) J Chem Phys 100:6046
22. Dhinojwala A, Hooker JC, Torkelson JM (1994) J Non-Cryst Solids 172–174:286
23. Qui T-C, Chikaki S, Kanato H (1994) Polymer 35:4465
24. Liu LY, Rankrishna D, Lachritz HS (1994) Macromolecules 27:5987
25. Wang CH, Guan HW, Gu SH (1994) J Non-Cryst Solids 172–174:705
26. Wang H, Jarnagin RC, Samulski ET (1994) Macromolecules 27:4705

27. Dirk CW, Devanathan S, Velez M, Ghebremichael F, Kuzyk MG (1994) Macromolecules 27:6167
28. Brower SC, Hayden LM (1995) J Polym Sci B 33:2391
29. Hooker JC, Torkelson JM (1995) Macromolecules 28:7683
30. Staring EGJ, Rikken GLJA, Seppen CJE, Nijhuis S, Venhuizen AHJ (1991) Polym Prep 32:118
31. Staring EGJ, Synthesis of Polyurethanes with NLO-active Sidegroups
32. Kremer F, Boese D, Meier G, Fischer EW (1989) Prog Colloid Polym Sci 80: 129
33. Kohlrausch F (1847) Pogg Ann Phys 12: 393
34 Kohlrausch F (1863) Pogg Ann Phys 29: 337
35. Williams G, Watts DC (1970) Trans Faraday Soc 73:3348
36 Burger C (1994) Dissertation thesis, Philipps-Universität Marburg
37. Palmer RG, Stein DL, Abrahams E, Anderson PW (1984) Phys Rev Lett 53:958
38. Bahar I, Erman B, Fytas G, Steffen W (1994) Macromolecules 27:5200
39. Schussler S, Richert R, Bässler H (1994) Macromolecules 27:4318
40. Richert R (1985) Chem Phys Lett 118: 534
41. Richert R (1989) In: Bässler (ed) Optical Technics to Characterize Polymer Systems 5th ed Elsevier Science Publishers, Amsterdam, p 71
42. Ishida Y, Yamafuji K (1961) Kolloid-Z 177:97
43. Ribelles JLG, Calleja RD (1984) J Macrom Sci Phys B 23:255
44. Ribelles JLG, Calleja RD (1985) J Polym Sci Polym Phys Ed 23:1297
45 Rehage G, Borchard W (1973) In: Haward RN (ed) The Physics of Glassy Polymers. Applied Science Publishers, London, p 54
46. Struik LCE (1978) Physical Aging of Amorphous Polymers and Other Materials. Elsevier Science, Amsterdam
47. Matsuoka S (1981) Polym Eng Sci 21: 907
48 Hutchinson JM (1995) Progr Polym Sci 20:703
49. Schmidt-Rohr K, Kulik AS, Beckham HW, Ohlemacher A, Pawelzik U, Boeffel C, Spiess HW (1994) Macromolecules 27:4733
50. Williams ML, Landel RF, Ferry JD (1955) J Am Chem Soc 77:3701
51. Baehr C, Glüsen B, Wendorff JH (1994) Macrom Rapid Com 15:327
52. Havriliak S, Negami S (1966) J Polym Sci 14:99
53. Zentel R, Strobl GR, Ringsdorf H (1985) Macromolecules 18:960
54. Williams G (1993) In: Thomas EL (ed) Structure and Properties of Polymers Vol 12. VCH, Weinheim, p 471